AFTERSHOCKS FROM LOCAL DATA

By Charley J. Langer, Jean P. Whitcomb, and Arturo Aburto Q.

INTRODUCTION

Aftershocks of the main event were monitored in two phases by single-component portable seismographs from February 9 to February 27. This study represents a combined effort by the U.S. Geological Survey and the Nicaraguan Instituto de Investigaciones Sismicas. Rapid deployment of portable instrumentation around the Motagua fault zone provides a data base for the first detailed aftershock investigation of a major earthquake (magnitude greater than 7.5) in Central America. Tectonic and seismic aspects of the main event and large aftershocks are discussed in other sections of the report (Spence and others, Person and others). The topic addressed here is hypocentral locations of a representative sample of locally recorded aftershocks and their relationship to primary and secondary faulting.

INSTRUMENTATION AND FIELD PROCEDURE

Aftershocks were recorded by portable, smoked-paper seismographs, each consisting of a vertical transducer, a high-gain amplifier, and a crystal-controlled clock. The seismograph recorded at a speed of 60 mm/min, and the trace separation was 1 mm, which allowed 48 hours of continuous operation. Precise time corrections were determined with an oscilloscope by comparing WWV radio time with recorder clock times during record changes. Clock drift did not exceed 20 ms/day. Seismograph magnifications generally ranged between 50,000 and 100,000 at 10 Hz. Amplifier gains were limited by the background noise at the sites, most of which were on unconsolidated soils and close to cultural noise sources. Because of the intense aftershock activity at many of the station locations, the peak-to-peak deflection of the recorder pen was limited to 10 mm.

A two-phase aftershock recording program was required because of the great length of fault rupture (more than 240 km), constraints imposed by the available logistical support, and the limited amount of seismograph equipment available. The phase I, or western, network (table 5) was installed on February 9 and 10 and extended approximately 95 km east-west between Sanarate and Chichicastenango. Another portable seismograph was installed in Guatemala City after the main event by personnel at the Observatorio Nacional. This network surrounded the western end of the Motagua fault zone and also encompassed many of the northeast-trending secondary faults in the vicinity of Guatemala City, Chimaltenango, and Tecpan. The phase I operation was terminated on February 17 when all seismographs, except those in Guatemala City, were removed.

During phase II, a much broader seismograph network was installed to the east between Guatemala City and Puerto Barrios (table 5). It covered about 225 km of the central and eastern segments of the Motagua fault and adjacent regions. On February 18, 19, and 20, seismographs were located at eight sites (table 5). The Puerto Barrios station was relocated at a site near La Piña on February 21 because of the high cultural background noise at Puerto Barrios. Phase II was completed on February 27 when all the instruments were retrieved.

DATA AND ANALYSIS

Several thousand aftershocks were recorded during the field investigation (fig. 21). The amount of seismic activity was greatest at the western end, near Tecpan and Chimaltenango, and did not noticeably diminish during the 8-day monitoring period of the western network. The unusually high level of observed seismicity in this area is not merely a function of station location or of time, that is, early in the aftershock sequence; the Tecpan-Chimaltenango region is unique to the total aftershock zone in terms of level of seismicity.

Arrival times were determined by using a low-power magnifier and were corrected for variations in distance between minute marks. S-phases were easily identifiable in many cases, often at two or

TABLE 5.—*List of seismograph stations occupied during this study*

Name	Symbol	Latitude (°N)	Longitude (°W)	Elevation (metres)	Period of operation
		Western network			
Chichicastenango	CCO	14.950	91.110	1,990	Feb. 9–Feb. 17
Tecpan	TEC	14.766	90.996	2,320	Feb. 9–Feb. 17
Joyabaj	JOY	14.990	90.804	1,400	Feb. 9–Feb. 17
Chimaltenango	CHM	14.635	90.818	1,760	Feb. 9–Feb. 17
El Chol	ELC	14.958	90.487	995	Feb. 9–Feb. 17
Guatemala City	GCG	14.586	90.533	1,497	Feb. 9–present
Palencia	PAL	14 664	90.361	1,310	Feb 10–Feb. 17
Sanarate	SAN	14.784	90.196	770	Feb. 10–Feb. 17
		Eastern network			
Guatemala City	GCG	14 586	90.533	1,497	Feb. 6–present
San Jeronimo	SJE	15.065	90.247	1,005	Feb. 18–Feb. 27
Jalapa	JAP	14.638	90.003	1,370	Feb. 18–Feb. 27
Teleman	TEL	15.339	89 744	65	Feb. 19–Feb. 27
Chiquimula	CML	14.801	89.533	360	Feb. 18–Feb. 27
Quiriguá	ARC	15.273	89.039	70	Feb. 18–Feb. 27
La Esmeralda	RIO	15.656	88.994	10	Feb. 20–Feb. 27
Vitalis	VIT	15.312	88.806	120	Feb. 18–Feb. 27
La Piña	FFF	15.600	88.608	40	Feb. 23–Feb. 27
Puerto Barrios	PTO	15.712	88.583	40	Feb. 20–Feb. 22

more stations for the same earthquake. Accuracy of most P-wave times is thought to be within ±0.1 s; the selected S-wave readings are believed accurate to ±0.20 s.

Seventy-eight hypocenters (table 6), most of which lie inside or very near to the margins of the temporary seismic networks, were determined by the HYPO71 computer program (Lee and Lahr, 1975). A measure of their solution quality is denoted by the symbol SQ and ranges between B (good) and D (poor). This SQ rating is dependent upon the number and accuracy of data, station distribution, and crustal velocities. All D-quality solutions are a few kilometres outside the network; otherwise they would be rated as B or C.

The average root-mean-square (RMS) errors of the travel-time residuals are 0.17 s, which implies that the random errors in reading the P- and S- arrivals account for most of the RMS errors. An average of the standard errors indicates hypocentral accuracies of about ±1.3 km in the horizontal plane and approximately ±2 km in the vertical plane. Although the standard errors may not represent actual error limits, particularly for hypocenters outside the seismograph net, S-phase data mitigate the possibility of gross mislocations. Any systematic location error or bias is most likely caused by the six-layer Managua velocity model of Brown, Ward, and Plafker (1973) used in the HYPO71 program. This model was employed in this study because of the absence of velocity data for interior Guatemala. Although the model is an assumed velocity structure for the Managua area, it is representative of volcanic terrane and therefore may be generally applicable to the Motagua fault zone west of long 90.5° W. To the east, where crystalline and marine sedimentary rocks are predominant (Bonis and others, 1970), increased velocities would be expected in the upper layers. The Managua model, however, is considered adequate for obtaining preliminary locations.

Because the peak-to-peak signal amplitudes were electronically clipped, local magnitudes, M_L, are estimated from the aftershock coda lengths (Lee and others, 1972). The lower magnitude threshold for hypocentral determinations using either the western or eastern network data is about 2.2. None of the larger aftershocks reported by Person, Spence, and Dewey (this report) occurred within a temporary seismograph net. The largest located event (magnitude 3.8) is approximately one order of magnitude below the limit for teleseismically locatable earthquakes in Central America.

RESULTS AND DISCUSSION

Aftershock epicenters are distributed along the Motagua Valley from the lowlands near the Gulf of Honduras westward to the Guatemalan highlands northeast of Lake Atitlán, a distance of some 300 km. A large number of located events occurred on secondary faults south of the Motagua fault and west of long 90.3° W. (fig. 22). Focal depths range from near surface to about 14 km. In particular, we note the following aspects:

1. The eastern terminus of the causal fault rupture is most likely defined by the cluster of 12 epicenters southeast of Puerto Barrios. The gen-

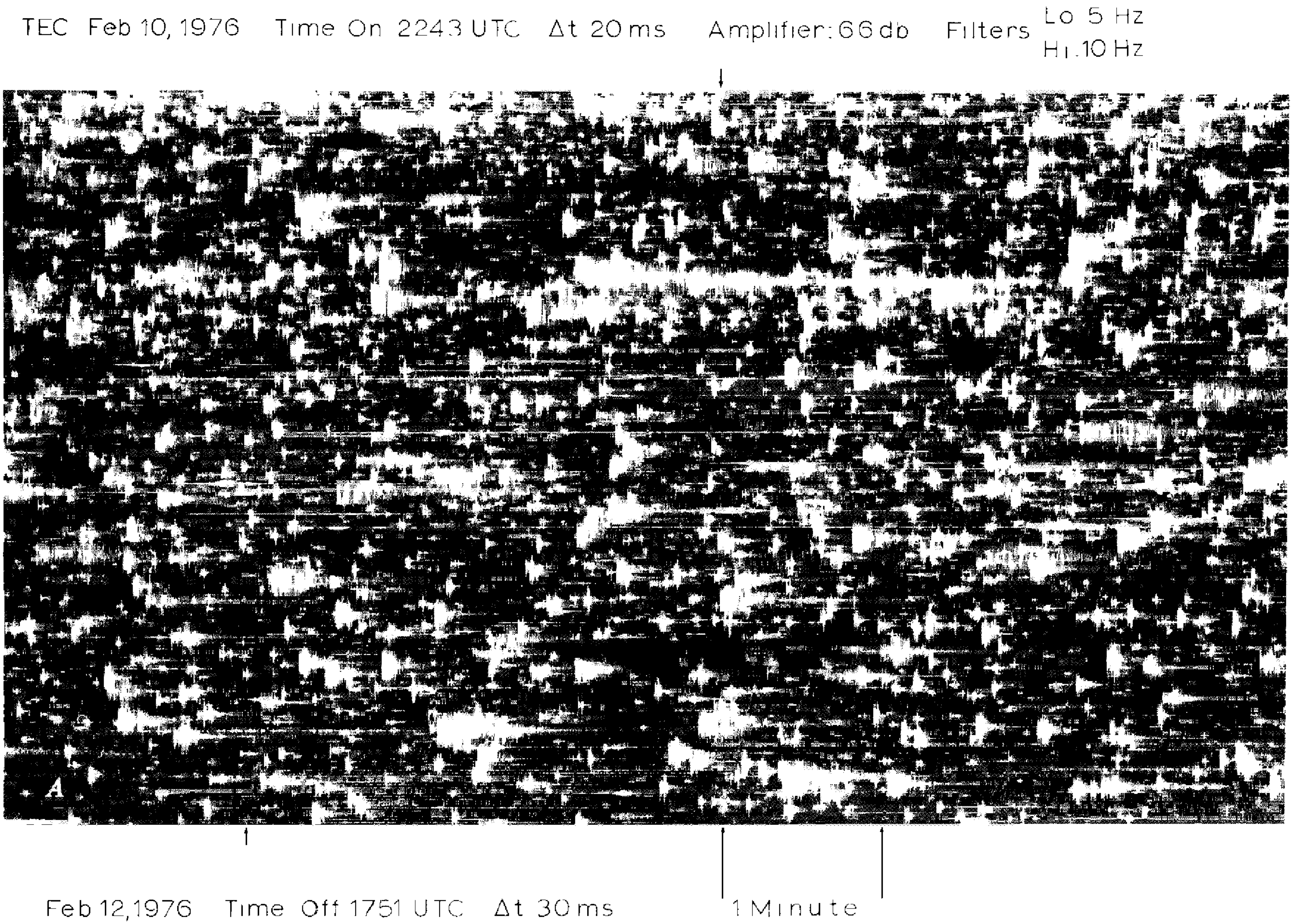

FIGURE 21.—Seismograms showing contrast of activity in the aftershock zone. Trace separation is 2 min, and minute marks are 60 mm apart on original records. *A*, Station TEC seismogram for February 10–12, 1976. *B*, Station VIT seismogram for February 25–27, 1976. Station location shown in figure 22. Station code is in the Glossary.

FIGURE 21.—Continued.

TABLE 6.—*Aftershocks of the main event located by temporary seismograph network*

[[1]No. sta.--refers to the number of stations used to obtain hypocentral solutions, [2]DMIN--distance to the closest seismograph station, [3]RMS--root mean square errors of travel time residuals; [4]Standard errors--refers to the indices of precision relating to the values and distribution of the unknown errors in the hypocentral solution where DLAT = error in latitude, DLON = error in longitude, and DZ = error in depth, [5]SQ--a measure that is intended to indicate the general reliability of the hypocentral solution where A = excellent epicenter, good focal depth; B = good epicenter, fair focal depth; C = fair epicenter, poor focal depth; D = poor epicenter, poor focal depth; [6]M_L--local magnitude of shock.]

	Western network											
								Standard errors[4]				
Date (Feb 1976)	Origin (UTC)	Lat. N (deg)	Long. W (deg)	Depth (km)	No.[1] sta	DMIN[2] (km)	RMS[3] (sec)	DLAT (km)	DLON (km)	DZ (km)	SQ[5]	M_L[6]
11	0636 48.69	14.750	91.126	9.2	8	14	0.18	1.1	1.3	1.5	C	3.2
11	0932 20.37	14.808	90.510	10.0	7	17	0.14	0.9	0.6	2.1	B	3.1
11	0953 02.55	14.760	90.980	7.0	7	2	0.11	0.6	0.8	1.2	B	2.9
11	1044 34.78	14.763	91.024	10.3	7	3	0.09	0.6	0.7	0.5	C	2.8
11	1051 03.91	14.767	90.975	4.2	7	2	0.19	1.5	1.5	1.5	B	2.9
11	1142 03.72	14.724	90.998	4.0	8	5	0.22	1.3	1.3	1.4	C	2.9
11	1636 23.01	14.790	90.984	4.9	7	3	0.04	0.3	0.3	0.4	B	3.0
11	2210 58.78	14.637	90.680	4.0	10	6	0.16	1.7	0.4	1.8	C	3.3
11	2253 51.55	14.809	90.596	2.0	7	20	0.24	0.4	0.3	1.2	C	2.4
12	0039 13.82	14.759	90.501	2.0	6	18	0.25	0.6	0.5	1.9	C	2.7
12	0144 35.11	14.861	90.343	12.2	7	18	0.20	1.9	1.7	2.4	C	2.6
12	0215 04.82	14.694	90.468	6.0	8	12	0.11	0.7	0.4	2.2	C	3.3
12	0333 36.40	14.855	90.710	12.0	9	18	0.21	0.9	0.7	1.6	B	2.7
12	0408 15.10	14.745	90.499	13.0	8	17	0.22	0.9	0.8	2.4	B	2.5
12	0439 54.52	14.636	90.668	12.1	7	16	0.11	1.1	0.4	1.4	C	3.0
12	0545 45.58	14.827	90.513	13.0	8	15	0.19	0.9	0.6	1.9	B	2.8
12	0702 02.43	14.859	90.340	10.5	8	14	0.11	0.8	0.5	1.3	B	3.3
12	0743 42.34	14.800	90.544	12.3	7	18	0.19	1.1	1.0	2.7	B	-
12	0744 35.68	14.852	90.619	12.2	9	18	0.25	1.0	0.7	4.3	B	3.0
12	1057 35.51	14.714	90.796	11.7	8	9	0.10	0.7	0.4	1.2	B	3.2
12	1203 33.49	14.589	90.625	13.2	7	21	0.09	1.0	0.4	1.0	C	3.2
12	1927 36.00	14.590	91.037	10.0	8	9	0.13	0.8	1.6	1.2	C	3.4
12	2211 59.01	14.674	90.482	12.0	7	13	0.20	0.9	1.0	2.4	C	2.4
12	2250 34.00	14.760	90.355	5.4	7	11	0.28	2.6	1.4	4.8	C	2.9
13	0627 42.32	14.673	90.483	10.0	7	13	0.16	0.7	0.8	5.3	C	3.1
13	0701 32.46	14.684	90.477	11.9	8	13	0.18	0.9	0.7	2.2	C	3.2
13	1344 01.31	14.755	90.987	5.7	8	1	0.16	1.0	2.3	1.7	C	3.2
13	2359 50.50	14.767	91.025	1.1	8	3	0.20	1.5	1.2	1.5	C	3.3

Western network													
								Standard errors[4]					
Date (Feb 1976)	Origin (UTC)	Lat. N (deg)	Long W (deg)	Depth (km)	No.[1] sta.	DMIN[2] (km)	RMS[3] (sec)	DLAT (km)	DLON (km)	DZ (km)	SQ[5]	M_L[6]
14	0300 40978	14.858	90.636	11.7	9	20	0.10	0.4	0.3	1.2	B	3.1
14	0315 59.79	14.696	90.545	10.0	8	20	0.20	0.9	0.8	2.8	C	3.2
14	0424 53.89	14.831	90.319	9.0	7	14	0.25	1.2	1.5	3.7	C	2.4
14	0916 38.15	14.711	90.737	10.7	9	12	0.17	1.0	0.7	2.1	B	3.1
14	1543 57.80	14.699	90.481	12.0	8	13	0.19	0.6	0.5	1.5	C	2.7
14	1757 33.16	14.700	90.514	12.4	8	17	0.32	1.6	1.6	3.7	C	3.2
14	1842 41.94	14.754	90.312	10.0	7	11	0.29	0.6	0.7	2.8	B	2.2
14	1912 53.22	14.643	90.950	4.0	8	14	0.14	1.2	0.8	0.8	C	3.8
14	2036 28.16	14.815	90.583	10.6	8	19	0.14	0.7	0.6	1.9	B	3.5
14	2044 04.68	14.743	90.377	6.0	8	9	0.24	0.7	0.8	3.5	B	3.1
14	2122 55.03	14.740	91.007	11.4	8	5	0.10	1.1	1.0	0.5	C	3.2
14	2219 24.40	14.746	90.355	8.0	7	9	0.24	0.5	0.6	1.6	B	2.8
14	2318 26.40	14.741	90.323	5.0	6	9	0.21	1.4	0.5	2.0	B	2.8
15	0034 43.75	14.776	90.965	6.2	9	1	0.15	0.6	0.6	1.6	B	3.4
15	0136 12.15	14.808	90.551	2.5	10	18	0.27	0.6	0.5	1.1	C	3.4
15	0650 51.18	14.728	90.359	2.5	8	7	0.24	0.8	0.9	2.7	B	2.4
15	1053 24.11	14.720	90.748	10.0	8	12	0.25	0.5	0.5	3.3	B	3.2
15	1308 31.57	14.782	90.980	6.4	9	2	0.10	0.6	0.5	0.9	B	3.4
15	2019 59.93	14.792	90.982	3.8	6	3	0.25	2.4	2.3	4.0	C	3.2
16	0758 08.62	14.848	90.678	12.2	11	21	0.16	0.7	0.4	1.1	B	2.9
16	0911 46.82	14.750	90.998	10.0	7	2	0.23	1.8	1.9	1.2	D	3.1
17	0345 47.31	14.708	91.008	7.8	6	6	0.04	0.5	0.5	0.5	C	2.8
17	0527 05.94	14.723	90.801	11.8	10	10	0.20	0.8	0.6	2.2	B	2.9
17	1549 25.34	14.791	90.974	2.4	6	4	0.09	1.2	0.8	1.4	B	2.9
20	0321 50.53	15.132	89.228	1.3	8	24	0.16	0.9	0.7	1.1	C	2.4
21	0203 36.01	15.052	89.452	5.9	7	29	0.18	1.0	1.0	4.0	C	3.1
21	0752 07.81	14.991	89.627	10.4	8	23	0.20	0.9	0.7	2.0	C	3.2
21	1303 52.99	14.971	89.676	11.2	6	24	0.08	0.5	0.5	1.2	B	2.9
22	0500 33.55	15.671	88.445	10.0	5	16	0.16	0.8	2.3	1.6	C	2.6
22	0642 40.71	15.526	88.520	8.5	6	22	0.07	0.7	1.5	5.5	D	2.9
22	1209 58.28	15.275	89.007	10.0	6	3	0.16	2.8	1.0	1.8	D	3.7
22	2138 32.95	15.217	89.003	14.0	7	7	0.16	1.5	0.8	0.9	C	3.8
23	0503 36.68	15.314	88.906	8.9	6	11	0.16	1.3	0.9	1.6	C	3.2
24	0417 00.95	15.670	88.437	10.0	5	20	0.21	0.6	1.4	1.1	C	2.7
24	0737 18.11	15.556	88.519	5.1	6	11	0.10	2.2	2.1	2.8	D	2.2

TABLE 6.—*Aftershocks of the main event located by temporary seismograph network*—Continued

Eastern network													
Date (Feb. 1976)	Origin (UTC)		Lat. N (deg)	Long. W (deg)	Depth (km)	No.[1] sta.	DMIN[2] (km)	RMS[3] (sec)	Standard errors[4] DLAT (km)	DLON (km)	DZ (km)	SQ[5]	M_L[6]
24	0807	06.51	14.983	89 635	8.5	8	23	0.11	0.3	0 4	1.6	B	2.7
24	0821	49.24	15.660	88.438	1.6	6	19	0 13	0.6	0 5	0.5	C	3.2
24	1316	05.14	15.485	88.601	10.0	5	13	0.20	0.6	0.9	2 6	C	2 5
24	1337	59.96	15.496	88.599	12.4	6	12	0.27	2.6	2.5	4.2	D	3.0
25	0128	48.30	14.977	89.674	5.9	7	25	0.13	0.3	0.4	1.2	B	3.3
26	0033	22.94	14.964	89.690	7.6	8	25	0.05	0.2	0.2	1.0	B	2.7
26	0510	13.27	15.617	88.437	7.0	5	18	0 19	1.0	0.8	1.1	C	2.4
26	1120	06.00	14.841	89.641	8.6	7	13	0.14	1 1	0 6	2.0	B	2.9
26	1903	20.29	15.561	88.515	8.0	6	11	0.21	0.5	1.1	2.1	C	2 3
26	2216	11.70	14 972	89.612	8.0	8	21	0.17	0.5	0.7	2.0	C	2.8
27	0120	58.22	15.580	88.451	9.0	5	17	0 05	0.9	1.0	1.0	C	3.1
27	0344	29.49	14 972	89.662	10.0	8	23	0 28	0.5	0 7	1.8	C	2.7
27	0458	00.86	15 537	88 565	2.8	5	8	0 14	0.4	3 3	2.8	D	2.5
27	1200	38.49	15.602	88.621	5.7	7	1	0 20	2.0	4.0	2 8	C	2.4

eral trend of the southern group of eight aftershocks is in line with the inferred extension of the Motagua fault (Plafker and others, this report), whereas the four epicenters slightly to the north may be associated with induced movement at the eastern end of the San Agustín fault.

2. Epicenters associated with the western end of the Motagua fault do not extend beyond the mapped fault breakage. Consequently, with the data at hand, the aftershock pattern does not suggest a more precise limit to the primary fault rupture than the obvious diminution of seismicity west of long 90.45° W. Also, there are no located aftershocks that appear to be related to induced movement on the western segment of the San Agustín fault.
3. The distribution of energy release along the Motagua fault proper is roughly uniform, with exception of the concentration of activity west of Zacapa. The group of seven epicenters between long 89.6° W. and 89.7° W. may be a result of fracturing east of where the Motagua fault bends from a general east-west direction to a northeasterly direction. Three northeast-trending secondary faults (not shown in fig. 22), which cut Paleozoic metamorphic rocks, are mapped in this area (Bonis and others, 1970)
4. The majority of aftershocks located west of long 90.3° W. are directly associated with secondary faulting. Four groups are considered to be of principal interest:
   a. Tecpan (long 91° W., lat 14.75° N.). The high level of activity observed at the Tecpan seismic station (fig. 21) is reflected by the dense cluster of epicenters located in this area. Plafker, Bonilla, and Bonis (this report) have defined a lineament that projects through Tecpan and the center of the northeasterly trending concentration of aftershocks. Therefore, on the basis of the epicentral locations, the lineament can be interpreted as a northeast-striking fault.
   b. Chimaltenango. Four epicenters occurring in the vicinity of a northeast-striking lineament that runs through Chimaltenango lend support to the existence of a secondary fault.
   c. Guatemala City region. These aftershocks are very likely associated with faults

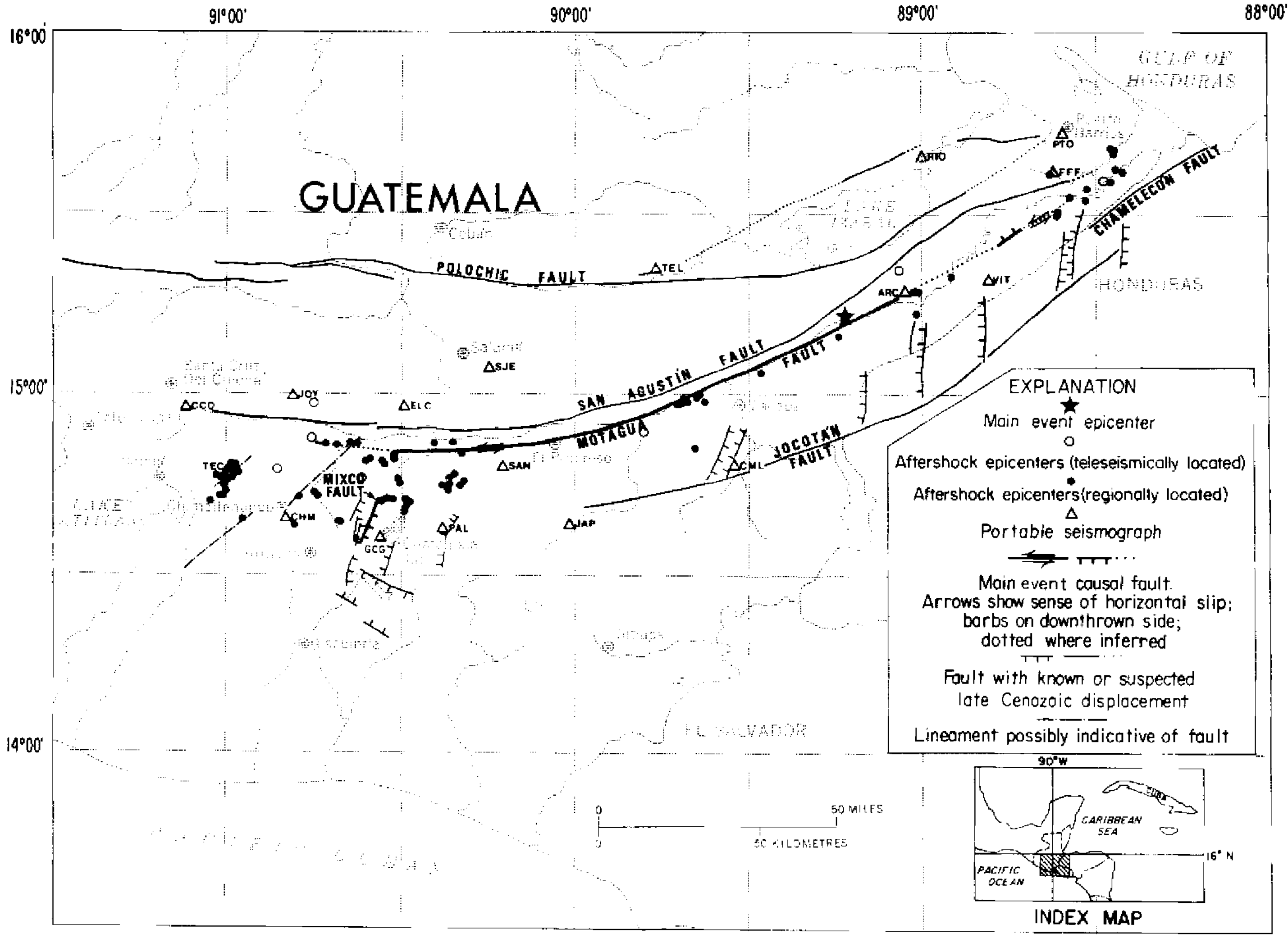

FIGURE 22.—Aftershock epicenters and portable seismograph locations (geology from Plafker and others, this report). See table 5 for station names and their geographical locations and table 6 for aftershock-location parameters. Station code is in the Glossary. (Base map modified from Guatemala, Instituto Geográfico Nacional, 1974, 1:500,000.)

forming the Guatemala City graben. The Mixco fault, west of the city, ruptured the ground surface. Some epicenters appear to correlate with the Mixco fault and also with the northerly extension of the mapped fault bounding Guatemala City on the southeast.

d. Agua Caliente (long 90.35° W., lat 14.75° N). A group of epicenters 15 km north of Palencia (station PAL) surround the Agua Caliente Bridge site. Secondary faulting, although not mapped at this locale, is certainly indicated by the aftershock cluster and may have contributed, in part, to the collapse of the bridge.

5. The preponderance of aftershocks lying off the Motagua fault west of long 90.3° W. suggests that induced motion along secondary faults is rare east of long 90.3° W.
6. There is an apparent southerly bias of epicentral locations along the Motagua fault proper. The spatial distribution of aftershocks thought to be associated with the primary fault indicates a systematic offset of 2 to 3 km. This offset would suggest that (1) the Motagua fault is dipping steeply to the south in accordance with the main-event focal mechanism of Dewey and Julian (this report) or (2) there is a large contrast in seismic velocities across the fault similar to that observed by Eaton, O' Neill, and Murdock (1970) on the San Andreas rift zone near Parkfield, California.